



Published in final edited form as:

Cerebellum. 2013 June ; 12(3): 377–389. doi:10.1007/s12311-012-0427-x.

Enhanced survival of wild type and Lurcher Purkinje cells in vitro following inhibition of conventional PKCs or stress-activated MAP kinase pathways

Hadi S. Zanjani^{1,2,*}, Ann M. Lohof^{1,2}, Rebecca McFarland^{4,6}, Michael W. Vogel^{4,5}, and Jean Mariani^{1,2,3}

¹CNRS, UMR7102, Paris F75005, France

²Université Pierre et Marie Curie-P6, UMR7102, Paris, F75005, France

³Hôpital Charles Foix, Institut de la Longévité, 94205 Ivry-Sur-Seine, France

⁴Maryland Psychiatric Research Center, Department of Psychiatry, University of Maryland School of Medicine, P.O. Box 21247, Baltimore, MD 21228

Abstract

Recent studies using both dissociated and organotypic cell cultures have shown that heterozygous Lurcher (*Lc/+*) Purkinje cells (PCs) grown in vitro share many of the same survival and morphological characteristics as *Lc/+* PCs in vivo. We have used this established tissue culture system as a valuable model for studying cell death mechanisms in a relatively simple system where neurodegeneration is induced by a constitutive cation leak mediated by the Lurcher mutation in the $\delta 2$ glutamate receptor (*GluR $\delta 2$*). In this study, Ca^{++} imaging and immunocytochemistry studies indicate that intracellular levels of Ca^{++} are chronically increased in *Lc/+* PCs and the concentration and/or distribution of the conventional PKC γ isoform is altered in degenerating *Lc/+* PCs. To begin to characterize the molecular mechanisms that regulate *Lc/+* PC death, the contributions of conventional PKC pathways and of two MAP kinase family members, JNK and p38, were examined in slice cultures from wild type and *Lc/+* mutant mouse cerebellum. Cerebellar slice cultures from P0 pups were treated with either a conventional PKC inhibitor, a JNK inhibitor, or a p38 inhibitor either from 0 to 14 or 7 to 14 DIV. Treatment with either of the three inhibitors from 0 DIV significantly increased wild type and *Lc/+* PC survival through 14 DIV, but only *Lc/+* PC survival was significantly increased following treatments from 7 to 14 DIV. The results suggest that multiple PC death pathways are induced by the physical trauma of making organotypic slice cultures, naturally-occurring postnatal cell death, and the *GluR $\delta 2^{Lc}$* mutation.

*Corresponding Author: Hadi Zanjani, Equipe Développement et Vieillessement du Système Nerveux, UMR NPA 7102 CNRS et Univ. P. & M. Curie, Case 14, 9, Quai St. Bernard, 75005, Paris, France.

⁵Current address: Division of Neuroscience and Basic Behavioral Science, National Institutes of Mental Health, 6001 Executive Blvd, Bethesda, Maryland 20892-9645

⁶Current address: Department of Biology, University of Maryland Baltimore County, Baltimore, Maryland 21201

Conflicts of Interest: The authors certify that there is no conflict of interest concerning the work presented in this manuscript.

This article was prepared while MWV was employed at the University of Maryland School of Medicine. The opinions expressed in this article are the author's own and do not reflect the view of the National Institutes of Health, the Department of Health and Human Services, or the United States government.

Keywords

Cell death; Lurcher mutant mouse; JNK; PKC; MAP Kinase; Organotypic culture; Purkinje cells; JNK

Introduction

Neurons actively enter cell death pathways both during development and in pathological processes. Identifying the precise mechanisms that regulate neuronal cell death is one of the fundamental goals in neurobiology. However, our understanding of cell death is hampered by the fact that multiple complex biochemical pathways are involved in the various modes of cell death. Thus, there is a need for well-defined and relatively simple models. This study is part of an overall analysis of the molecular mechanisms of cell death in Purkinje cells (PCs) in the *Lc/+* mutant as a relatively simple model of neuronal death caused by a well-defined lesion in a single, well-characterized cell type.

Lurcher (gene symbol, *Lc*) is a gain-of-function point mutation in the $\delta 2$ glutamate receptor gene that turns the receptor (GluR $\delta 2$) into a constitutively open cation channel (1, 2). GluR $\delta 2$ receptors are predominantly expressed in cerebellar PCs, and the leak current mediated by the GluR $\delta 2^{Lc}$ receptor chronically depolarizes cerebellar PCs starting during the first postnatal week of development (3). In the heterozygous *Lc/+* mutant almost all PCs degenerate after the first week of postnatal life via pathways that have been described as either apoptotic, autophagic, or necrotic (2–7). Homozygous *Lc* mutants die around birth subsequent to massive neuronal cell loss in the hindbrain during embryonic development (8).

A general hypothesis guiding our studies of PC death in the GluR $\delta 2^{Lc/+}$ mutant is that chronic depolarization of PCs mediated by the GluR $\delta 2^{Lc}$ leak current affects a wide range of cellular homeostatic systems, including key signaling pathways that are important in the regulation of PC dendritic development and cell death. Genetic studies have indicated that there are likely to be multiple apoptotic molecular pathways that can contribute to GluR $\delta 2^{Lc/+}$ PC death. For example, one hallmark of apoptotic GluR $\delta 2^{Lc/+}$ PC death is the up-regulation of procaspase-3 expression in many *Lc/+* PCs, and the expression of activated caspase-3 in PCs that appear to be degenerating. Deletion of the pro-apoptotic gene *Bax* can transiently delay GluR $\delta 2^{Lc/+}$ PC death, but in *Lc/+;Bax^{-/-}* double mutants, activated caspase-3 can no longer be detected, suggesting that an alternative cell death pathway has been invoked in the absence of *Bax* expression (9, 10). Other recent studies have shown evidence for an increase in oxidative stress in GluR $\delta 2^{Lc/+}$ PCs (11), which may lead to the deleterious activation or suppression of a number of cellular developmental or homeostatic pathways.

The purpose of this study is to investigate the role of three critical protein kinase pathways associated with cellular responses to stress on the survival and differentiation of chronically depolarized and stressed GluR $\delta 2^{Lc/+}$ PCs. The three pathways investigated are the conventional, Ca^{2+} -activated, phospholipid-dependent protein kinases (cPKC) and the stress related MAPK pathways represented by the downstream effectors, c-Jun N-terminal kinase (JNK) and p38. The family of conventional PKC isoforms are involved in signal transduction systems associated with cell proliferation, differentiation, and apoptosis, and they are highly sensitive to the redox status of their environment (reviewed in (12)). JNK and p38 are downstream kinases in a sequence of MAPK signaling cascades that are associated with a variety of stressors, including inflammation, activation of death receptors, apoptosis, and oxidative stress (reviewed in (13, 14)). Activation of the stress activated JNK

pathway, for example, is thought to induce apoptosis by transcription-dependent or – independent mechanisms. With the aid of selective inhibitors for the conventional PKCs, JNK, and p38, we show that treatment of WT and *Lc/+* cerebellar organotypic slice cultures with Gö6976 (cPKC inhibitor), SP600125 (JNK inhibitor) or SB 203580 (p38 inhibitor) significantly increases both GluR $\delta 2^{+/+}$ and GluR $\delta 2^{Lc/+}$ PC survival *in vitro*. These results suggest that activation of all three pathways is associated with PC death processes *in vitro* related to the stress of slicing and culturing tissue, normal developmental neuronal cell death, and the homeostatic stress of chronic depolarization mediated by the GluR $\delta 2^{Lc}$ mutant receptor.

Materials and Methods

Animals

GluR $\delta 2^{Lc/+}$ mutant and wild type (GluR $\delta 2^{+/+}$) pups were generated by mating B6CBACa A^{w-J}/A-Grid2^{Lc/J} males with wild type B6CBA females from Janvier Laboratories or Jackson Laboratories (NB: Grid2 is the official name of the *Lc* gene). Males were harem mated with one male to two or three females and the females were checked for copulatory plugs every day the mice remained together. The day of finding the copulatory plug was considered embryonic day 0.5 (E0.5) and the day of birth is counted as postnatal day 0 (P0). All animals were housed in standard conditions (14 hours light, 10 hours dark) in animal facilities either at the Université Pierre et Marie Curie (UPMC) or the Maryland Psychiatric Research Center (MPRC) and provided with food and water *ad libitum*. The animal facility at the UPMC is fully accredited by the French Research and Higher Education ministry, and studies were conducted in accordance with the Guide for Care and Use of Laboratory Animals provided by the guidelines established by “le comité national d’éthique pour les sciences de la vie et de la santé.” The animal facilities at the MPRC are fully accredited by the American Association for the Accreditation of Laboratory Animal Care (AAALAC) and the studies were conducted in accordance with the Guide for Care and Use of Laboratory Animals provided by the NIH.

The *Lc/+* or *+/+* genotype of P0 pups was identified by PCR and single-stranded conformation polymorphism (SSCP) as described previously (3). GluR $\delta 2$ S1 and AS primers were used to amplify a stretch of DNA that spans the single base pair change in the Grid2^{Lc} mutation (15).

Organotypic tissue slice cultures

Cerebellar slices were prepared from GluR $\delta 2^{Lc/+}$ mutant and GluR $\delta 2^{+/+}$ pups at P0. Pups were decapitated and the brain removed in ice cold Gey’s balanced salt solution with 5 mg/mL glucose. The cerebellum was separated from the rest of the brain with forceps after removing the choroid plexus and dura. The entire cerebellum was then sliced into 350 μ m sagittal sections, and the slices were placed on the membrane of Millicell CM inserts (Millipore, MA). All of the sections from one cerebellum were arranged on one culture insert. Slices were maintained at the interface between the air and the culture media consisting of 50% Basal Medium Eagle (BME), 25% Hank’s Balanced Salt Solution (HBSS), 25% heat inactivated horse serum, 1 mM L-glutamine, and 5 mg/ml D-glucose in a humidified chamber with 5% CO₂ (pH 7.3) at 35° C. The media was changed every 2–3 days and cultures were fixed at 14 days *in vitro*. JNK inhibitor SP600125, P38 inhibitor SB 203580 or PKC inhibitor Gö6976 were added in the culture medium either from DIV 1 or DIV 7. All of the *in vitro* organotypic experiments with cerebellar slices were conducted at the Université Pierre et Marie Curie, including the Ca⁺⁺ imaging and electrophysiology studies.

Immunohistochemistry

Slice cultures were fixed in 4% paraformaldehyde in 0.1M phosphate buffer (pH 7.4) for 30 minutes at room temperature followed by multiple washes with 10 mM phosphate buffered saline (0.9% NaCl, PBS). Slices were then incubated for 1 hour in PBS containing 0.2 % Triton X-100, 0.2% gelatin, 0.1M lysine before immunostaining with mouse monoclonal antibodies against calbindin (dilution 1:5000, Swant, Bellinzona, Switzerland). Antibodies were revealed with CY3- conjugated Donkey anti-mouse antibody (1:500 dilutions, Jackson ImmunoResearch Laboratories, Inc). After 2 h incubation in buffer containing the secondary antibody, the slices were washed several times with PBS and counterstained with DNA fluochrome Hoechst 33258 (diluted 1/50000, Sigma) and mounted in Mowiol (Calbiochem, La Jolla, CA, USA).

For immunocytochemistry in fixed cerebellar sections, mouse pups were euthanized by cardiac perfusion with 0.9% saline followed by 4% paraformaldehyde (while deeply anesthetized with Euthasol, >100 $\mu\text{g/g}$). Following the perfusion, brains were removed from the skull, postfixed for 2 hours in fresh fixative, and then cryoprotected with 20% sucrose in 10 mM phosphate buffered saline (PBS). At least 48 h later, the fixed brains were embedded in OCT and frozen in isopentane. Fixed, frozen brains were cut at 12 μm on a Leica cryostat, collected directly on slides, and stored at -70°C until stained. To prepare slides for immunofluorescence studies, slides were rinsed in 10mM PBS, followed by incubation in two changes of 0.1M glycine for 5 min each. Endogenous fluorescence was reduced by incubating the sections in 50 mM ammonium chloride for 1 hour. The sections were then rinsed three times in 10mM PBS and incubated for an hour in blocking solution containing 3% normal goat serum and 0.3% Triton X-100. Sections were then incubated in the following primary antibodies overnight at 4°C : mouse monoclonal anti-PKC γ (Zymed: 1/100) and rabbit polyclonal anti-calbindin (Sigma: 1/1000) or rabbit polyclonal anti-activated caspase-3 (R&D: 1/500). The following day, sections were rinsed 3 times in PBS and then incubated for 2 hours with fluorescent-labeled secondary antibodies (anti-mouse or anti-rabbit Alexa 594 and Alexa 488: Molecular Probes: 1/200). After incubation, they were rinsed once in 10mM PBS and incubated with 300nM DAPI, then rinsed 3 times in 10 mM PBS, once in distilled water, and coverslipped with gelmount. The finished slides were then photographed using a Zeiss Axioplan fluorescence microscope with an Olympus DP70 CCD camera. All immunofluorescence experiments included slides (wild type and *Lc/+*) with no primary antibody incubation as a control for non-specific immunolabeling. Digital images were cropped and adjusted using Adobe Photoshop for color balance and intensity. All of the immunohistochemistry studies on cerebellar sections from brains fixed *in vivo* were performed at the Maryland Psychiatric Research Center.

PC counts

In most cases, the total number of PCs per culture was directly determined by systematically scanning the entire culture area and counting all fluorescent calbindin-labeled PCs. The cell counts were conducted with a 40x objective and an eyepiece graticule was used to systematically sweep across the culture and to keep track of counted and uncounted areas. For cerebellar slice cultures treated with Gö6976 it was not possible to count all of the PCs since the density and total number was too high. Instead, the total number of PCs per slice was estimated from sampling the density of PCs and measuring the total area of each slice. The total area of the slices per culture was calculated by photographing each cultured slice and then measuring the area of the slice with Image-Pro 4.5 (Media Cybernetics, Maryland). The PC density was estimated in each slice by counting the number of PCs in $180 \times 180 \mu\text{m}$ grids systematically randomly selected throughout each slice. The total number of PCs per slice was then calculated as the product of the PC density and slice area. The total number of PCs was estimated as the sum of PCs in all of the slices cultured from each whole

cerebellum. The average number and density of PCs is reported as the mean \pm standard error.

Calcium imaging and electrophysiology

Standard patch-clamp recordings were used to determine the size of leak currents in GluR $\delta 2^{+/+}$ and GluR $\delta 2^{Lc/+}$ PCs either from slice cultures from 8–16 DIV, or from acute slices prepared from pups aged P8–P11 using standard procedures (16). Cerebellar slices were placed in artificial CSF (aCSF) containing (in mM) 125 NaCl, 25 NaHCO₃, 10 glucose, 3.5 KCl, 1.25 NaH₂PO₄, 2 CaCl₂, and 1 MgCl₂ and oxygenated with 95%:5% O₂:CO₂. Slices are incubated at 32–34°C for at least 1 h until ready for recording. For the recordings, slices were placed in a chamber mounted on an Olympus BX51-WI microscope, and continuously perfused with aCSF at 2 ml/min. Whole-cell configuration was acquired with glass pipettes containing a 0.125% Neurobiotin solution containing (in mM) 115 K gluconate, 10 HEPES, 2 MgCl₂, 20 KCl, 2 MgATP, 2 Na₂-ATP, and 0.3 GTP (pH 7.3, 280 \pm 5 mOsm). Electrophysiological recordings were acquired with an Axopatch 200B amplifier (Axon Instruments), digitized, and analyzed using Acquis (Biologic, France).

Leak current was measured for each PC. For measurements of Ca⁺⁺ levels, individual PCs in acute slice preparations were patch clamped and filled with Fura (100 μ M). Fluorescence levels were measured using a CCD camera (Cascade 1K, Photometrics) piloted by the Metamorph image program at 340 and 380 nm to calculate 340nm/380nm ratios as a measure of the basal intracellular Ca⁺⁺ concentration. In some experiments, a brief depolarizing voltage step was applied to the PC to evaluate the time course and amplitude of increased Ca⁺⁺ concentration.

Statistical analysis

The number of surviving PCs in drug-treated and control GluR $\delta 2^{Lc/+}$ and GluR $\delta 2^{+/+}$ slice cultures was initially analyzed with two-way analysis of variance (ANOVA) including genotype and drug treatment as co-variants (StatView 5.0, Cary, North Carolina). A log transformation of the number of PCs per culture was used to stabilize the variance for the ANOVA analysis. Post-hoc comparisons between groups were made using the Bonferroni/Dunn test.

For the statistical analysis of Ca⁺⁺ levels using 340n/380nm fluorescence ratios, the non-parametric Mann-Whitney U test was used to compare the differences between Ca⁺⁺ levels. ANOVA was used to compare mean leak currents in GluR $\delta 2^{Lc/+}$ and GluR $\delta 2^{+/+}$ PCs.

Results

Intracellular Ca⁺⁺ levels in *Lc/+* PCs

To test whether intracellular Ca⁺⁺ levels are affected by the GluR $\delta 2^{Lc}$ leak current, individual PCs in acute slice preparations were patch clamped and filled with Fura-2 (100 μ M). Fluorescence levels were measured at 340 and 380 nm to calculate the basal [Ca⁺⁺] as 340nm/380nm ratios. Pseudo-color is used to show fluorescence intensity in a filled WT PC at 340 nm (Fig. 1A) and for the 340nm/380nm ratio (Fig. 1B). The labeling is much less intense than in an equivalent *Lc/+* PC (Fig. 1C, D) where the filled *Lc/+* PC body and dendrites can be seen in the 340nm/380nm ratio image. Comparison of *Lc/+* and wild type PCs at P8–12 shows that intracellular Ca⁺⁺ levels are increased in resting *Lc/+* PCs compared with wild type PCs (Fig. 1E; Mann-Whitney test, $p < 0.0001$).

In addition to increased basal levels of Ca⁺⁺, voltage clamp studies indicate that *Lc/+* PCs do not have a normal Ca⁺⁺ response to depolarization (Fig. 1F). WT and *Lc/+* PCs were

voltage clamped at -60 mV in acute cerebellar slices at P8–11 and then given a test depolarizing pulse (to -10 mV for 50 msec) and changes in the 340nm/380nm fluorescence ratio measured. Wild type PCs respond with a robust Ca^{++} increase ($n=13$; representative response shown in red) but *Lc/+* PCs do not show any response to the depolarizing pulse ($n=6$, representative response shown in blue). The lack of a Ca^{++} response in *Lc/+* PCs is likely due to the abnormally high basal levels of Ca^{++} .

Thus our Ca^{++} imaging results show that resting levels of Ca^{++} are constitutively increased in *Lc/+* PCs, which could cause activation of the conventional PKC isoforms.

Altered expression of PKC γ in *Lc/+* PCs

To test the hypothesis that chronic increases in resting Ca^{++} levels may affect the expression patterns of conventional PKC isoforms, we have focused our studies on the expression of PKC γ , the PKC isoform with the highest and most uniform expression levels in cerebellar PCs. Cerebellar PCs express a wide range of PKC isoforms, although the exact complement is disputed (17). There is some agreement, though, that PCs express the conventional PKCs (cPKC), alpha (α) and gamma (γ), and the novel PKCs (nPKC), delta (δ) and epsilon (ϵ). The developmental distribution of PKC γ was qualitatively analyzed in PCs in WT and *Lc/+* PCs in cerebellar sections from pups at P10, P15, and P25 using immunocytochemistry (ICC) with an anti-PKC γ antibody from Invitrogen. The pattern and level of ICC labeling for PKC γ is similar in WT and *Lc/+* cerebellar slices at P10 (data not shown), but by P15 the intensity of PKC γ immunolabeling is reduced in most *Lc/+* PCs compared with WT PCs (Fig. 2) and by P25 PKC γ immunolabeling has virtually disappeared in *Lc/+* PCs (data not shown). However, at P15 there are distinct heterogeneities in PKC γ staining among the *Lc/+* PCs. Figure 2 shows epifluorescence double-labeling for PKC γ (green) and calbindin (red: a marker for PCs) in P15 WT and *Lc/+* cerebellar sections at the same antibody concentration and at the same photographic exposure times. The overall intensity of immunolabeling for PKC γ is reduced in the *Lc/+* PCs (Fig. 2: D–F) compared with WT PCs (Fig. 2: A–C), which may indicate that PKC γ levels decline in the *Lc/+* PCs. There are some exceptions, however, where the intensity of PKC γ immunolabeling is increased compared with other *Lc/+* PCs (arrows and arrowheads in Fig. 2: D–F). In some cases, the morphology of these intensely-labelled *Lc/+* PCs does not differ from the other *Lc/+* PCs (arrowheads in Fig. 2 D–F), but in other cases they have the characteristic appearance of *Lc/+* PCs during degeneration (arrows in Fig. 2: D–F). These observations suggest that the overall levels of PKC γ may be reduced in depolarized *Lc/+* PCs, but they also raise the possibility that the expression or distribution of PKC γ may undergo a change in *Lc/+* PCs as they actually degenerate.

To explore the possibility that *Lc/+* PCs with more intense PKC γ immunolabeling are degenerating, a small sample of P15 *Lc/+* cerebellar slices were double labeled with antibodies to PKC γ (Fig. 3 A; green) and activated caspase-3 (Fig. 3 B; red). In general, *Lc/+* PCs that express activated caspase-3 have more rounded and stumpy dendrites that are often associated with calbindin-positive blebs that look like dendrites that have broken off the rest of the PC ((6) and unpublished observations). As shown in Fig. 3, many of the degenerating *Lc/+* PCs expressing activated caspase-3 also stained more intensely for PKC γ (lower arrow), but this was not always the case (upper arrow). While a quantitative analysis of the distribution and intensity of PKC γ immunolabeling in *Lc/+* PCs that express activated caspase-3 was outside the scope of this project, these qualitative descriptions raise the possibility that the expression or distribution of PKC γ may be altered in *Lc/+* PCs that are actively degenerating and that PKC γ activation could play a role in the *Lc/+* cell death pathway.

***Lc/+* and WT PC survival *in vitro* is enhanced by treatment with a conventional PKC inhibitor, Gö6976**

The family of PKC kinases plays a critical role in signaling pathways in stressed cells (12), and conventional PKC (cPKC) isoforms are stimulated by Ca^{++} . Since Ca^{++} signaling is disrupted in *GluR82^{Lc/+}* PCs and the expression and/or distribution of PKC γ appears to be altered in *Lc/+* PCs *in vivo*, we tested the hypothesis that activation of cPKC isoforms contributes to *GluR82^{Lc/+}* PC death by treating *GluR82^{+/+}* and *GluR82^{Lc/+}* cerebellar slice cultures with the general conventional PKC inhibitor, Gö6976 (1 μ M), from 0 to 14 DIV. The total number of calbindin-labeled PCs was then counted or calculated at 14 DIV. These experiments were conducted *in vitro* since it was not feasible to consistently inhibit cPKC activity selectively in the *in vivo* cerebellum with pharmacological tools and *Lc/+* PC differentiation and survival *in vitro* appears to recapitulate their *in vivo* development in key aspects (18).

Previous studies have shown that after 14 DIV in control slice cultures, *GluR82^{Lc/+}* Purkinje survival is reduced by over 70% compared to control values (18). However, treating cultures with the PKC inhibitor Gö6976 from 0 DIV dramatically increased PC survival in both *GluR82^{+/+}* and *GluR82^{Lc/+}* slice cultures at 14 DIV (Fig. 4A–D). Cultures from 54 P0 pups were treated with Gö6976 or vehicle, and a random sample was selected for PC counts (Fig. 4E). ANOVA analysis of the resulting counts showed that there were significant effects of genotype and treatment (Genotype: ANOVA, $F_{2,51}=46.0$, $p < 0.0001$; Treatment: ANOVA, $F_{2,51}=93.3$, $p < 0.0001$). The results of the PC counts indicate that treatment with 1 μ M Gö6976 resulted in a 6 fold increase in the number of surviving WT PCs by 14 DIV (Treated: $14,490 \pm 585$, $n=7$ vs. control: 2216 ± 266 , $n=10$; $p < 0.0001$) and an over 20 fold increase in the number of surviving *GluR82^{Lc/+}* PCs per cerebellar slice culture (Treated: $14,780 \pm 1054$, $n=7$ vs. control: 625 ± 65 , $n=13$, $p < 0.0001$). There is no significant difference between the numbers of surviving PCs in treated control or *GluR82^{Lc/+}* cultures ($p > 0.5$), suggesting that treatment with Gö6976 restores *GluR82^{Lc/+}* PC survival to the level of wild type cerebellar slice cultures also treated with Gö6976.

While treatment with Gö6976 from 0 DIV dramatically increases both *GluR82^{+/+}* and *GluR82^{Lc/+}* PC survival, the mechanism is unknown so it was not clear that Gö6976 treatment was affecting PC death due to the *GluR82^{Lc}* leak current. *In vivo*, PC death due to the *GluR82^{Lc}* mutation in the *GluR82* receptor is not apparent until approximately 1 week after birth, and a similar delay in *GluR82^{Lc/+}* PC death is also observed in slice and isolated cell cultures (18). To test the hypothesis that cPKC activation contributes specifically to *GluR82^{Lc/+}* PC death *in vitro*, in a separate set of experiments *GluR82^{+/+}* and *GluR82^{Lc/+}* PC slice cultures were treated with Gö6976 (1 μ M) from 7 to 14 DIV (Fig. 4E). Delayed treatment of cerebellar slice cultures from 7 DIV only increased the number of surviving wild type PCs 1.5 fold ($3,706 \pm 495$; $n=9$), while *GluR82^{Lc/+}* PC survival increased by about three fold ($1,858 \pm 170$; $n=8$) compared with untreated cerebellar slice cultures. However, the increase in PC survival following Gö6976 treatment from 7 to 14 DIV is still significant for both *GluR82^{+/+}* and *GluR82^{Lc/+}* PCs ($p < 0.002$).

Previous studies have shown that blocking the *GluR82^{Lc/+}* leak current with 1-naphthylacetylspermine (NASP), a channel blocker for Ca^{++} permeable iGluRs, also restores *GluR82^{Lc/+}* PC survival to *in vitro* wild type levels (although WT PC survival is not affected by NASP treatment: (18)). To determine whether Gö6976 treatment increases *GluR82^{Lc/+}* PC survival by eliminating the leak current, a series of cerebellar slice cultures were treated with Gö6976 (1 μ M) until 14 DIV. The *GluR82^{Lc}* – mediated leak current was then measured in PCs from Gö6976 treated and untreated *GluR82^{+/+}* and *GluR82^{Lc/+}* PC slice cultures. For technical reasons Gö6976 could not be included in the electrophysiological bath solution. Since cerebellar slices were rinsed in the

electrophysiological aCSF for at least an hour before recordings were made, the drug is likely to have washed out at the time of the experiments. However, as shown in Figure 4F there are no significant differences in the magnitude of the leak current between treated and untreated *Lc/+* PCs. There is a significant effect of genotype, with the *Lc/+* PCs having significantly higher leak currents compared to WT controls (ANOVA $F_{3,84} = 13.187$, $p < 0.0001$). The results indicate that treatment with Gö6976 does not permanently eliminate the leak current mediated by the $\text{GluR}\delta 2^{Lc}$ channel. While we cannot rule out the possibility that the continuous presence of Gö6976 might have had an effect on the leak current, there is no evidence that Gö6976 acts on glutamate channels. Instead we hypothesize that Gö6976 is acting downstream of the leak current to block activation of one or more cell death pathways following the activation of cPKC isoforms.

PC survival following treatments with inhibitors for the stress-related MAP kinases JNK and p38

The MAP kinases JNK and p38 are critical downstream effector kinases for signaling pathways involved in the cellular response to various types of oxidative stress. To compare the effects of a cPKC inhibitor on $\text{GluR}\delta 2^{+/+}$ and $\text{GluR}\delta 2^{Lc/+}$ PC survival with the effects of JNK and p38 inhibitors, wild type and *Lc/+* cerebellar slice cultures were treated from 0 to 14 DIV with either the JNK II inhibitor SP600125 or the p38 inhibitor SB 203580 (Fig. 5). Counts of calbindin-labeled $\text{GluR}\delta 2^{+/+}$ and $\text{GluR}\delta 2^{Lc/+}$ PCs at 14 DIV treated with the JNK inhibitor SP600125 (10 μM) from 0 DIV indicate there were significant effects of genotype (ANOVA, $F_{1,41} = 65.21$; $p < 0.0001$) and treatment (ANOVA, $F_{2,41} = 79.42$, $p < 0.0001$) on PC survival, but no significant genotype-by-treatment interactions ($p > 0.1$; Fig. 5G). In wild type cultures, SP600125 treatment significantly increased $\text{GluR}\delta 2^{+/+}$ PC survival by almost 500% (Treated: $10,855 \pm 774$, $n=5$ vs. control: 2216 ± 266 , $n=10$; $p < 0.0001$), while in *Lc/+* slice cultures, $\text{GluR}\delta 2^{Lc/+}$ PC survival increased by about 675% (Treated: $4,205 \pm 407$; $n=7$ vs. control: 625 ± 65 ; $n=13$; $p < 0.0001$).

As in the study of PKC inhibition, to address the concern that that treatment of cerebellar slice cultures with SP600125 (10 μM) from the first day of culture through 14 DIV is non-specifically reducing PC loss from the stress of being placed in slice cultures or rescuing PCs from developmental cell death, wild type and *Lc/+* cerebellar slice cultures were also treated with SP600125 (10 μM) from 7 to 14 DIV (Fig. 5G). This delayed treatment schedule did not significantly affect the number of surviving wild type PCs at 14 DIV ($2,851 \pm 563$ (SP600125-treated), $n=6$ vs. 2216 ± 266 (non-treated), $n=10$, $p > 0.05$), but $\text{GluR}\delta 2^{Lc/+}$ PC survival increased by approximately 230% in the treated cultures ($1,460 \pm 318$, $n=6$ vs. 625 ± 65 , $n=13$; $p < 0.0005$). A similar treatment of wild type and *Lc/+* cerebellar slices from 7 DIV with the highly selective peptide JNK inhibitor, DJNKII, produced similar findings of increased $\text{GluR}\delta 2^{Lc/+}$ PC survival (19), but no effect on wild type PC survival. In the current study, among the *Lc/+* slice cultures, treatment with SP600125 (10 μM) starting from 0 DIV significantly increased $\text{GluR}\delta 2^{Lc/+}$ PC survival compared with treatment starting at 7 DIV ($p < 0.001$). This could mean that some $\text{GluR}\delta 2^{Lc/+}$ PCs start dying before P7 or that early treatment with the JNK inhibitor increases the overall initial survival of PCs in slice culture, leading to relatively higher PC survival at 14 DIV, assuming that the rate of cell death is the same.

Treatment of wild type and *Lc/+* cerebellar slice cultures with the p38 inhibitor SB 203580 (10 μM) from 0 to 14 DIV also had significant treatment and genotype effects on PC survival (Fig. 5H: Genotype: ANOVA, $F_{1,75} = 77$, $p < 0.001$; Treatment: ANOVA, $F_{2,75} = 30.85$, $p < 0.0001$) with no significant interactions ($p > 0.1$). The number of surviving WT PCs was increased by about 2-fold following SB 203580 treatments (4359 ± 470 , $n=4$ vs. 2005 ± 215 , $n=10$; $p < 0.0005$) and *Lc/+* PC survival was increased by over 3-fold (2192 ± 290 , $n=8$ vs. 593 ± 54 , $n=13$; $p < 0.0001$). When cerebellar slice cultures were treated

with SB 203580 from 7 to 14 DIV, there was no significant change in the number of GluR82^{+/+} PCs (2719±355) compared with untreated WT cultures (2005±215 PCs, $p > 0.1$). However, there was still an almost 2-fold increase in the number of GluR82^{Lc/+} PCs (1081 ± 188) compared with untreated *Lc/+* cerebellar cultures (593±54 PCs, $p < 0.005$).

Low-power magnification photomicrographs of wild type and *Lc/+* untreated cultures and those treated with the JNK II inhibitor (SP600125) or the p38 inhibitor (SB 203580) confirm the quantitative results (Fig. 5A–F). The density of calbindin-labeled PCs is greater in the *Lc/+* cultures treated with the JNK II and p38 inhibitors compared with controls and many of the pharmacologically treated *Lc/+* cerebellar slices look more like normal cerebellar slices with PCs arranged in distinct lobules sending axons to what looks like the deep cerebellar nuclei.

GluR82^{Lc/+} PC dendritic differentiation is not affected by treatment with inhibitors for PKC, JNK, or p38

The treatment of cerebellar slice cultures with the pharmacological inhibitors for cPKCs and the MAP kinases JNK and p38 all resulted in significant increases in both GluR82^{+/+} and GluR82^{Lc/+} PC survival. However, the images of the dendritic trees of GluR82^{Lc/+} PCs in the treated slice cultures indicates that exposure to either the cPKC, JNK, or p38 inhibitors does not reverse the phenotype of deficient dendritic growth in GluR82^{Lc/+} PCs (Fig. 6). GluR82^{Lc/+} PC dendrites in all of the treated *Lc/+* slice cultures showed decreased dendritic growth and complexity compared with treated and control GluR82^{+/+} PC dendrites. In their general appearance, the dendrites of *Lc/+* PCs treated with Gö6976, SP600125, or SB 203580 may even appear less well differentiated and stunted compared with untreated *Lc/+* PCs (compare Fig. 6B with 6D, F, and H). PC morphology was not quantified in this study, however, because of concerns it would not be possible to differentiate the effects of increased PC packing density in the treated cultures with the direct effects of the inhibitors on individual PCs.

Discussion

The results of this study demonstrate that treating cerebellar slice cultures with the kinase inhibitors Gö6976, SP600125, or SB 203580 from 0 to 14 DIV dramatically increases both GluR82^{+/+} and GluR82^{Lc/+} PC survival, although the inhibitors do not appear to stimulate the differentiation of GluR82^{Lc/+} PC dendrites. Treatment of the cultures with the inhibitors starting at 7 DIV also rescues significant numbers of GluR82^{Lc/+} PCs, with a much less dramatic affect on the survival of wild type PCs. The results suggest that the activation of conventional PKC isoforms, JNK, and p38 are all involved in the mechanisms for PC death in cerebellar slice cultures in general, and in the mechanisms of GluR82^{Lc/+} PC in particular. Inhibiting the activation of cPKCs, JNK, or p38 starting at the time when the slice cultures are established may reduce the overall PC death that is due to the stress of sectioning the cerebellum and placing the slices in culture, and may even have an effect on naturally occurring PC death in the slice cultures. However, we hypothesize that the decrease in GluR82^{Lc/+} PC death following treatment with any of the three kinase inhibitors starting from 7 DIV is due to the inhibition of cell death pathways involved in excitotoxic *Lc/+* PC death.

Previous studies of wild type and *Lc/+* PC death *in vivo* and *in vitro* have presented immunohistochemical evidence for the expression of phosphorylated c-Jun in wild type and *Lc/+* PCs as a marker for activation of the JNK kinases during periods of PC death (19, 20). In this study, we present qualitative evidence for potential changes in the density or distribution of PKC γ in *Lc/+* PCs, as reflected in changes in the intensity of immunolabeling for PKC γ at P15 and P25. In most *Lc/+* PCs at P15, the intensity of PKC γ

immunolabeling is reduced compared with controls, but in a few cases the intensity is increased. While we recognize that the intensity of immunofluorescence should be interpreted cautiously as an indicator for protein expression or concentration changes (there could be many factors that influence the intensity of labeling beyond changes in the concentration of the antigen, e.g. changes in antigen accessibility as a cell degenerates), one possible interpretation of this observation is that there is an increase in PKC γ protein or a change in its distribution (indicating activation) in a small subset of *Lc/+* PCs at a given time at P15. This raises the intriguing possibility that PKC γ expression or activation is dynamic in *Lc/+* PCs and at some point in the life/death history of *Lc/+* PCs, cPKC isoforms are activated and this leads to their rapid death. Since the period of PC death in *Lc/+* mutants *in vivo* (and *in vitro*) extends over a fairly long period it is statistically likely that only a few *Lc/+* PCs will be in the process of dying at a given time point (the time of perfusion). This would account for the observation that only a few *Lc/+* PCs immunolabel for activated caspase-3 in P15 cerebella *in vivo* (9, 10). Gö6976 may dramatically increase *Lc/+* PC survival *in vitro* because it prevents *Lc/+* PC death when cPKC isoforms are activated at some point as they begin to degenerate. However, it is not at all clear what triggers the death of individual *Lc/+* PCs over the course of the period of PC death in the *Lc/+* cerebellum, especially since the available electrophysiological evidence suggests that all *Lc/+* PCs are chronically depolarized by the end of the first week of postnatal development and blocking the GluR $\delta 2^{Lc}$ leak current rescues *Lc/+* PCs, at least *in vitro* (3, 18). There is some evidence that heterogeneity in the expression of neuroprotective factors in PC compartments may influence the timing of *Lc/+* PC death (see (21, 22)).

In cerebellar slice cultures taken from P1 to P5 pups, Dusart and colleagues have shown that there is enhanced PC death at these ages that may correspond to a postnatal period of developmental PC death (19, 23–27). As shown by Western blots, the JNK and p38 kinases are also activated in wild type cerebellar slice cultures, though p38 appears to be activated early in response to the physical disruption of the slices being put in culture while JNK activity appears to be associated with programmed cell death in the slice culture (26). In results similar to the current study, treatment of wild type P3 cerebellar slice cultures with the PKC inhibitor Gö6976, the JNK inhibitor D-JNKII, or the p38 inhibitor SB 203580 for 5 DIV significantly increased the survival of PCs (24, 26). In a separate study (19), treatment of wild type and *Lc/+* cerebellar slice cultures from P0 pups with the selective JNK II inhibitor, D-JNKII, from 7 to 14 DIV significantly increased *Lc/+* PC survival, but not wild type PC survival.

In this study, we have not directly analyzed the activation of any of the conventional PKCs, JNK, or p38, in wild type or *Lc/+* PCs so our interpretation of the data depends on the specificity of the drug treatments. In the slice culture experiments, we deliberately used low concentrations of both SP600125 and SB 203580 (10 μ M), that have been reported to be selective for the JNK 1–3 and p38 α and β isoforms, respectively (28, 29). Gö6976 is reported to be a potent and selective inhibitor for conventional PKC isoforms (30, 31), but there is also evidence that Gö6976 has an equal affinity for inhibition of TrkA and TrkB neurotrophin receptors (32). In their study of the effects of Gö6976 on PC survival and axonal regeneration, Ghomari et al. (24) demonstrated, using L7-PKCI transgenic mice (33), that the increased survival of PCs following treatment with Gö6976 was likely to be due to direct inhibition of cPKC isoforms and not due to the inhibition of Trk receptors. Since we observed similar results with Gö6976 with respect to PC survival, we hypothesize that Gö6976 is acting through inhibition of one or more of the conventional PKC isoforms. There is agreement in the literature that rodent PCs express the conventional α and γ PKC isoforms, while the I and II isoforms may only be expressed by granule cells (although there are some disagreements in the literature because of potential cross-reactivity of antibodies: see (17, 34, 35)). Qualitative evidence is presented here for changes in the pattern of

immunolabeling for PKC γ in *Lc/+* PCs in vivo, but our results do not indicate which cPKC isoforms are activated in *Lc/+* PCs and whether one or all are primarily responsible for activating cell death pathways.

PKC activity in PCs is necessary for the induction of long-term depression at PC-parallel fiber synapses, the elimination of multiple climbing fiber innervation, and the differentiation of PC dendritic trees (17, 36–38). The elimination of supernumerary climbing fibers from PCs also involves activation of the GluR δ 2 and mGluR1 receptors and Ca⁺⁺-dependent activation of PKC (17). In this case, deletion of PKC γ interferes with climbing fiber elimination so this isoform may play a key role in activity dependent mechanisms (38). Similarly, PKC γ may play a key role in the activity-dependent regulation of PC dendritic differentiation; stimulation of PKC activity reduces PC growth in vitro while PKC inhibition promotes dendritic differentiation (17). PC dendritic growth in vitro is enhanced in PKC γ knock-out mice and PCs in slice cultures from PKC γ deficient mice do not respond to PKC inhibitors with enhanced dendritic growth (39). Based on these results, the activation of cPKC isoforms by increased intracellular Ca⁺⁺ levels in *Lc/+* PCs may play a role in the failure of *Lc/+* PC dendrites to differentiate normally. However, treatment with the cPKC inhibitor, Gö6976, at levels that prevents significant amounts of *Lc/+* PC cell death is not sufficient to restore *Lc/+* dendritic development, suggesting that there may be additional factors that control dendritic differentiation.

Activation of PKC isoforms is also associated with the induction of apoptosis in a variety of neurodegenerative diseases, from cerebral ischemia and reperfusion injury to Alzheimer's disease (31, 40–42). The interactions between PKC isoforms and apoptosis pathways are complex and, to a certain degree, cell type and stimulus specific. Yet in general PKC α , β , ϵ and ζ are often associated with suppression of apoptosis, while PKC δ is a critical pro-apoptotic signal in many cell types. PKC δ is activated by a variety of apoptotic stimuli including oxidative stress, death receptors, and by cleavage with activated caspase-3 (41). Cleavage of PKC δ by caspase-3 creates a constitutively active enzyme that serves both as a marker and effector of apoptosis. Oxidative stress can have differential effects on PKC activity, with low levels of reactive oxygen or reactive nitrogen stimulating PKC activity while higher concentrations can inhibit PKC activity, although high ONOO⁻ concentrations can also increase intracellular protease activity which leads to proteolytic activation of PKC isoforms (42–45).

A recent study (46) presented evidence that the key stimulus for cell death mediated by the GluR δ 2^{Lc} channel is the influx of Na⁺ ions and a subsequent decrease in ATP levels. Ionic stress caused by the increase in intracellular Na⁺ and Ca⁺⁺ levels in *Lc/+* PCs can lead to a variety of changes in intracellular homeostasis, and one of the most important of these could be the increased production of reactive oxygen species (ROS) that can interact with nitric oxide (NO) to form reactive nitrogen species (RNS). We hypothesize that the initiation of cell death processes in *Lc/+* PCs is strongly dependent on oxidative stress and the production of RNS caused by the ionic imbalance from the constitutive GluR δ 2^{Lc} Na⁺ leak. Among many possibilities, protein oxidation or nitration by RNS can cause the activation of various PKC isoforms and the p38 and JNK/c-Jun pathways (14, 42–45, 47). Activation of PKC isoforms can trigger the production of even more ROS and direct activation of cell death pathways (12). Phosphorylation of c-Jun by JNK may activate a number of target genes, including the cell death promoters Fas-L and Bim, leading to stimulation of apoptotic cell death pathways. Furthermore, activation of the p38 and JNK pathways can also suppress activity in the ERK pathway that promotes cell survival (13). It is important to note that there are multiple complex biochemical interactions that are responsible for regulating a cell's response to stress and many of the interactions may be cell-type specific, depending on the matrix of protein expression within a particular cell. This may be particularly true for

cerebellar PCs which are known to have heterogeneous patterns of protein expression in cerebellar compartments that may affect cell death processes (21, 22). The timing of *Lc/+* PC death may ultimately depend on a complex interaction among pro- and anti-death factors with individual PCs.

In this study, treatment of wild type and *Lc/+* cerebellar slices with Gö6976 had a much more dramatic effect on cell survival than did the treatments with the JNK and p38 inhibitors. One possible interpretation of this result is that activation of cPKC isoforms is earlier in the web of interactions that lead to *Lc/+* PC death, so inhibiting cPKC activation is able to rescue more *Lc/+* PCs from cell death. However, we do not yet know the extent to which the PKC, JNK, and p38 pathways were inhibited by the pharmacological treatments, since the drug doses were chosen to preserve specificity as much as possible, but not to maximize inhibition of a particular pathway. Yet the present results provide strong support for the hypothesis that there are multiple pathways for wild type and *Lc/+* PC cell death. The magnitude of *Lc/+* PC rescue following treatment with Gö6976 from 0 to 14 and 7 to 14 DIV is the largest that we have observed in vivo or in vitro (e.g. 9, 10, 19, 20, 48) and suggests that activation of PKC isoforms play a key role in *Lc/+* PC death. Likewise, the dramatic increase in wild type PC survival following treatment with Gö6976 from 0 to 14 DIV indicates that activation of PKC isoforms also plays an important role in developmental PC death and in death due to the stress of being placed in tissue culture. The challenge is now to identify all of the molecular components of the web that regulates PC survival and death and to define the mechanisms by which they interact.

Acknowledgments

This work was supported by a NIH grant NS 34309 to M.W.V. and J.M. and by funds from “Centre National de la Recherche Scientifique” (CNRS) and Universite Pierre et Marie Curie; LIA (Laboratoire Internationaux Associé) grant from UPMC. MV was recipient of a visiting professorship grant from UPMC. We thank Fabrice Machulka for his assistance in animal breeding. We gratefully acknowledge the considerable contribution of Dr Pauline Cavalier in data acquisition. We thank the Cell Imaging and Flow Cytometry facility of the IFR83 (Paris, France) for access and technical support in microscopy.

References

1. Vogel MW, Caston J, Yuzaki M, Mariani J. The Lurcher mouse: Fresh insights from an old mutant. *Brain Res.* 2007; 1140:4–18. [PubMed: 16412991]
2. Yue Z, Horton A, Bravin M, DeJager PL, Selimi F, Heintz N. A novel protein complex linking the delta 2 glutamate receptor and autophagy: implications for neurodegeneration in lurcher mice. *Neuron.* 2002; 35(5):921–33. [PubMed: 12372286]
3. Selimi F, Lohof AM, Heitz S, Lalouette A, Jarvis CI, Bailly Y, et al. Lurcher GRID2-Induced Death and Depolarization Can Be Dissociated in Cerebellar Purkinje Cells. *Neuron.* 2003; 37(5):813–9. [PubMed: 12628171]
4. Dumesnil-Bousez N, Sotelo C. Early development of the Lurcher cerebellum: Purkinje cell alterations and impairment of synaptogenesis. *Journal of Neurocytology.* 1992; 21:506–529. [PubMed: 1500948]
5. Norman DJ, Feng L, Cheng SS, Gubbay J, Chan E, Heintz N. The lurcher gene induces apoptotic death in cerebellar Purkinje cells. *Development.* 1995; 121(4):1183–93. [PubMed: 7743930]
6. Selimi F, Doughty M, Delhaye-Bouchaud N, Mariani J. Target-related and intrinsic neuronal death in Lurcher mutant mice are both mediated by caspase-3 activation. *J Neurosci.* 2000; 20:992–1000. [PubMed: 10648704]
7. Wullner U, Loschmann P-A, Weller M, Klockgether T. Apoptotic cell death in the cerebellum of mutant *weaver* and *lurcher* mice. *Neurosci. Lett.* 1995; 200:109–112.
8. Cheng SS, Heintz N. Massive loss of mid- and hindbrain neurons during embryonic development of homozygous lurcher mice. *J Neurosci.* 1997; 17(7):2400–7. [PubMed: 9065501]

9. Selimi F, Vogel MW, Mariani J. Bax inactivation in Lurcher mutants rescues cerebellar granule cells but not Purkinje cells or inferior olivary neurons. *J Neurosci*. 2000; 20(14):5339–45. [PubMed: 10884318]
10. Doughty ML, De Jager PL, Korsmeyer SJ, Heintz N. Neurodegeneration in Lurcher mice occurs via multiple cell death pathways. *J Neurosci*. 2000; 20(10):3687–94. [PubMed: 10804210]
11. McFarland R, Blokhin A, Sydnor J, Mariani J, Vogel MW. Oxidative stress, nitric oxide, and the mechanisms of cell death in Lurcher Purkinje cells. *Devel Neurobio*. 2007; 67:1032–1046.
12. Giorgi C, Agnoletto C, Baldini C, Bononi A, Bonora M, Marchi S, et al. Redox control of protein kinase C: cell- and disease-specific aspects. *Antioxid Redox Signal*. 2010; 13(7):1051–85. [PubMed: 20136499]
13. Junttila MR, Li SP, Westermarck J. Phosphatase-mediated crosstalk between MAPK signaling pathways in the regulation of cell survival. *FASEB J*. 2008; 22(4):954–65. [PubMed: 18039929]
14. Shen HM, Liu ZG. JNK signaling pathway is a key modulator in cell death mediated by reactive oxygen and nitrogen species. *Free Radic Biol Med*. 2006; 40(6):928–39. Epub 2005 Nov 21. [PubMed: 16540388]
15. Zuo J, De Jager PL, Takahashi KA, Jiang W, Linden DJ, Heintz N. Neurodegeneration in Lurcher mice caused by mutation in 2 glutamate receptor. *Nature*. 1997; 388:769–773. [PubMed: 9285588]
16. Letellier M, Demais V, Bailly Y, Sherrard RM, Mariani J, Lohof AM. Reinnervation of late post-natal Purkinje cells by climbing fibres: neosynaptogenesis without transient multi-innervation. *Journal of Neuroscience*. 2007; 27:5373–5383. [PubMed: 17507559]
17. Metzger F, Kapfhammer JP. Protein kinase C: its role in activity-dependent Purkinje cell dendritic development and plasticity. *Cerebellum*. 2003; 2(3):206–14. [PubMed: 14509570]
18. Zanjani HS, McFarland R, Cavalier P, Blokhin A, Gautheron V, Levenes C, et al. Death and survival of heterozygous Lurcher Purkinje cells in vitro. *Dev Neurobiol*. 2009; 69(8):505–17. [PubMed: 19294643]
19. Repici M, Zanjani HS, Gautheron V, Borsello T, Dusart I, Mariani J. Specific JNK inhibition by D-JNKI1 protects Purkinje cells from cell death in Lurcher mutant mouse. *Cerebellum*. 2008; 7(4): 534–8. [PubMed: 18949529]
20. Lu W, Tsirka SE. Partial rescue of neural apoptosis in the Lurcher mutant mouse through elimination of tissue plasminogen activator. *Development*. 2002; 129(8):2043–50. [PubMed: 11934869]
21. Armstrong CL, Duffin CA, McFarland R, Vogel MW. Mechanisms of compartmental purkinje cell death and survival in the lurcher mutant mouse. *Cerebellum*. 2010; 10(3):504–14. [PubMed: 21104177]
22. Duffin CA, McFarland R, Sarna JR, Vogel MW, Armstrong CL. Heat shock protein 25 expression and preferential Purkinje cell survival in the Lurcher mutant mouse cerebellum. *J Comp Neurol*. 2010 In press.
23. Ghomari AM, Wehrle R, Bernard O, Sotelo C, Dusart I. Implication of Bcl-2 and Caspase-3 in age-related Purkinje cell death in murine organotypic culture: an in vitro model to study apoptosis. *Eur J Neurosci*. 2000; 12(8):2935–49. [PubMed: 10971635]
24. Ghomari AM, Wehrle R, De Zeeuw CI, Sotelo C, Dusart I. Inhibition of protein kinase C prevents Purkinje cell death but does not affect axonal regeneration. *J Neurosci*. 2002; 22(9): 3531–42. [PubMed: 11978830]
25. Ghomari AM, Dusart I, El-Etr M, Tronche F, Sotelo C, Schumacher M, et al. Mifepristone (RU486) protects Purkinje cells from cell death in organotypic slice cultures of postnatal rat and mouse cerebellum. *Proc Natl Acad Sci U S A*. 2003; 100(13):7953–8. Epub 2003 Jun 16. [PubMed: 12810951]
26. Repici M, Wehrle R, Antoniou X, Borsello T, Dusart I. c-Jun N-terminal kinase (JNK) and p38 play different roles in age-related Purkinje cell death in murine organotypic culture. *Cerebellum*. 2010; 10(2):281–90. [PubMed: 21191679]
27. Marin-Teva JL, Dusart I, Colin C, Gervais A, van Rooijen N, Mallat M. Microglia promote the death of developing Purkinje cells. *Neuron*. 2004; 41(4):535–47. [PubMed: 14980203]

28. Bennett BL, Sasaki DT, Murray BW, O'Leary EC, Sakata ST, Xu W, et al. SP600125, an anthrapyrazolone inhibitor of Jun N-terminal kinase. *Proc Natl Acad Sci U S A*. 2001; 98(24): 13681–6. [PubMed: 11717429]
29. Bain J, Plater L, Elliott M, Shpiro N, Hastie CJ, McLauchlan H, et al. The selectivity of protein kinase inhibitors: a further update. *Biochem J*. 2007; 408(3):297–315. [PubMed: 17850214]
30. Martiny-Baron G, Kazanietz MG, Mischak H, Blumberg PM, Kochs G, Hug H, et al. Selective inhibition of protein kinase C isozymes by the indolocarbazole Go 6976. *J Biol Chem*. 1993; 268(13):9194–7. [PubMed: 8486620]
31. Bright R, Mochly-Rosen D. The role of protein kinase C in cerebral ischemic and reperfusion injury. *Stroke*. 2005; 36(12):2781–90. Epub 2005 Oct 27. [PubMed: 16254221]
32. Behrens MM, Strasser U, Choi DW. Go 6976 is a potent inhibitor of neurotrophin-receptor intrinsic tyrosine kinase. *J Neurochem*. 1999; 72(3):919–24. [PubMed: 10037462]
33. De Zeeuw CI, Hansel C, Bian F, Koekkoek SK, van Alphen AM, Linden DJ, et al. Expression of a protein kinase C inhibitor in Purkinje cells blocks cerebellar LTD and adaptation of the vestibulo-ocular reflex. *Neuron*. 1998; 20(3):495–508. [PubMed: 9539124]
34. Hirono M, Sugiyama T, Kishimoto Y, Sakai I, Miyazawa T, Kishio M, et al. Phospholipase Cbeta4 and protein kinase Calpha and/or protein kinase CbetaI are involved in the induction of long term depression in cerebellar Purkinje cells. *J Biol Chem*. 2001; 276(48):45236–42. Epub 2001 Sep 10. [PubMed: 11551922]
35. Naik MU, Benedikz E, Hernandez I, Libien J, Hrabe J, Valsamis M, et al. Distribution of protein kinase Mzeta and the complete protein kinase C isoform family in rat brain. *J Comp Neurol*. 2000; 426(2):243–58. [PubMed: 10982466]
36. Leitges M, Kovac J, Plomann M, Linden DJ. A unique PDZ ligand in PKCalpha confers induction of cerebellar long-term synaptic depression. *Neuron*. 2004; 44(4):585–94. [PubMed: 15541307]
37. Metzger F, Kapfhammer JP. Protein kinase C activity modulates dendritic differentiation of rat Purkinje cells in cerebellar slice cultures. *Eur J Neurosci*. 2000; 12(6):1993–2005. [PubMed: 10886339]
38. Kano M, Hashimoto K, Chen C, Abeliovich A, Aiba A, Kurihara H, et al. Impaired synapse elimination during cerebellar development in PKC gamma mutant mice. *Cell*. 1995; 83:1223–1231. [PubMed: 8548808]
39. Schrenk K, Kapfhammer JP, Metzger F. Altered dendritic development of cerebellar Purkinje cells in slice cultures from protein kinase Cgamma-deficient mice. *Neuroscience*. 2002; 110(4):675–89. [PubMed: 11934475]
40. Alkon DL, Sun MK, Nelson TJ. PKC signaling deficits: a mechanistic hypothesis for the origins of Alzheimer's disease. *Trends Pharmacol Sci*. 2007; 28(2):51–60. [PubMed: 17218018]
41. Reyland ME. Protein kinase Cdelta and apoptosis. *Biochem Soc Trans*. 2007; 35:1001–1004. [PubMed: 17956263]
42. Steinberg SF. Structural basis of protein kinase C isoform function. *Physiol Rev*. 2008; 88(4): 1341–78. [PubMed: 18923184]
43. Lin D, Takemoto DJ. Oxidative activation of protein kinase Cgamma through the C1 domain. Effects on gap junctions. *J Biol Chem*. 2005; 280(14):13682–93. [PubMed: 15642736]
44. Knapp LT, Kanterewicz BI, Hayes EL, Klann E. Peroxynitrite-induced tyrosine nitration and inhibition of protein kinase C. *Biochem Biophys Res Commun*. 2001; 286(4):764–70. [PubMed: 11520063]
45. Chakraborti T, Das S, Chakraborti S. Proteolytic activation of protein kinase Calpha by peroxynitrite in stimulating cytosolic phospholipase A2 in pulmonary endothelium: involvement of a pertussis toxin sensitive protein. *Biochemistry*. 2005; 44(13):5246–57. [PubMed: 15794661]
46. Nishiyama J, Matsuda K, Kakegawa W, Yamada N, Motohashi J, Mizushima N, et al. Reevaluation of Neurodegeneration in lurcher Mice: Constitutive Ion Fluxes Cause Cell Death with, Not by, Autophagy. *J Neurosci*. 2010; 30(6):2177–87. [PubMed: 20147545]
47. Brown GC. Nitric oxide and neuronal death. *Nitric Oxide*. 2010; 23(3):153–65. [PubMed: 20547235]

48. Zanjani H, Rondi-Reig L, Vogel M, Martinou JC, Delhaye-Bouchaud N, Mariani J. Overexpression of a Hu-bcl-2 transgene in Lurcher mutant mice delays Purkinje cell death. *C R Acad Sci III*. 1998; 321(8):633–40. [PubMed: 9769861]

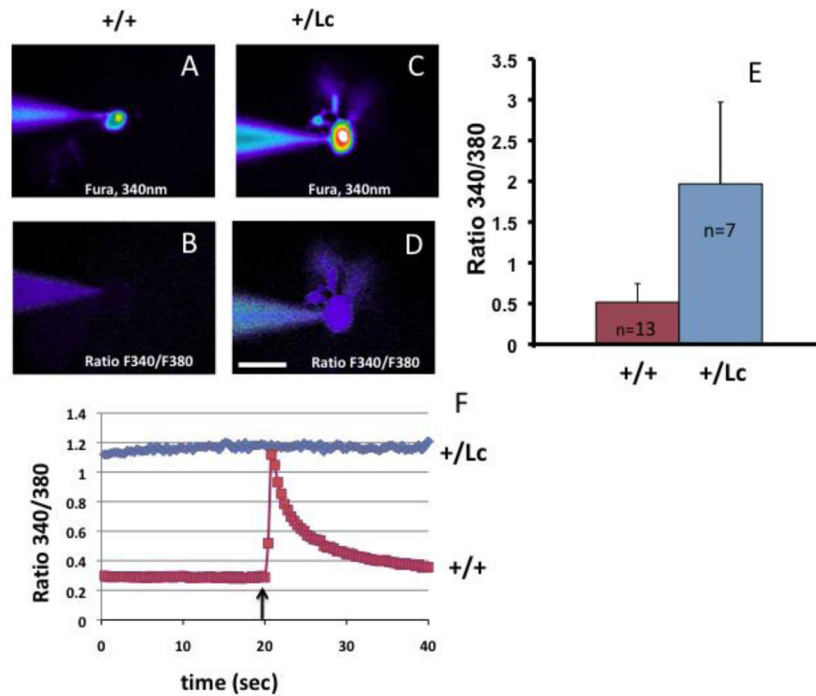


Figure 1. Elevated calcium concentrations in *Lc/+* PCs. Fura-2 imaging of WT (A–B) and *Lc/+* (C–D) PCs, measured by the ratio of fluorescence intensity at 340/380nm. The patch clamp electrode used to fill the cells is shown touching the cells from the left. Scale bar 20 μm. E. Mean fluorescence ratio for WT and *Lc/+* PCs. F. Representative ratiometric recordings of voltage clamped PCs show that resting basal Ca^{++} levels in *Lc/+* PCs are higher than in WT PCs and the *Lc/+* PCs do not respond to a step depolarizing pulse (arrow) with an increase in Ca^{++} levels as in WT PCs.

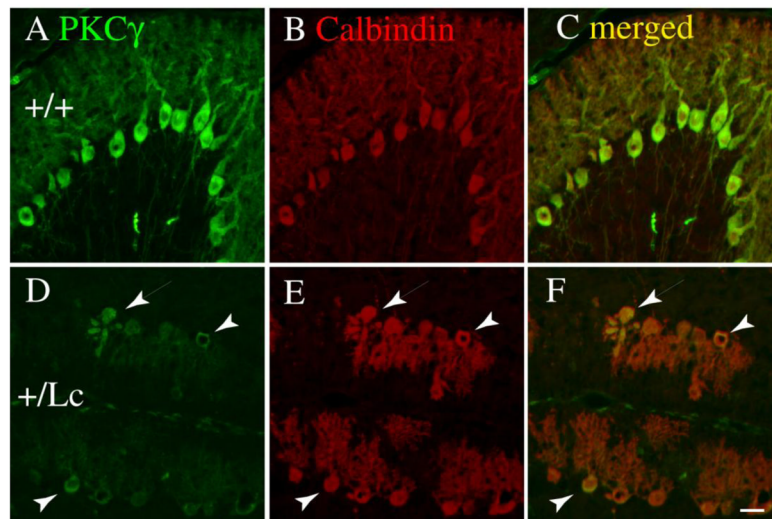


Figure 2. Double immunolabeling for PKC γ (green; A, D) and calbindin (red; B, E) in WT (AC) and *Lc/+* (D–F) in P15 cerebellar slices indicates that PKC γ is expressed in WT and *Lc/+* PCs, although the intensity of PKC γ immunolabeling is highly variable in *Lc/+* PCs. The images were taken at the same exposure settings. The merged images (C, F) were created by overlaying the original images in Adobe Photoshop, and no other editing was performed. Scale bar 20 μ m.

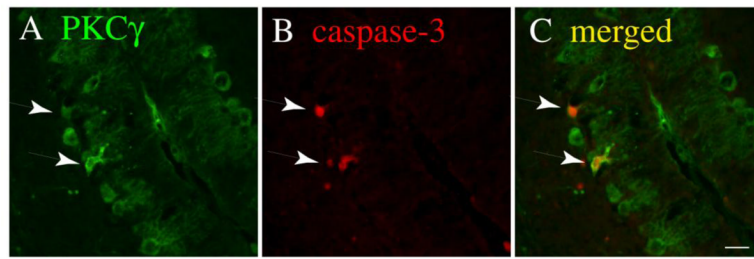


Figure 3. Double immunolabeling for PKC γ (green; A) and activated caspase-3 (red; B) in P15 *Lc/+* cerebellar slices indicates that PKC γ is expressed in degenerating *Lc/+* PCs. The merged image (C) was created by overlaying the original images in Adobe Photoshop. Scale bar 20 μm .

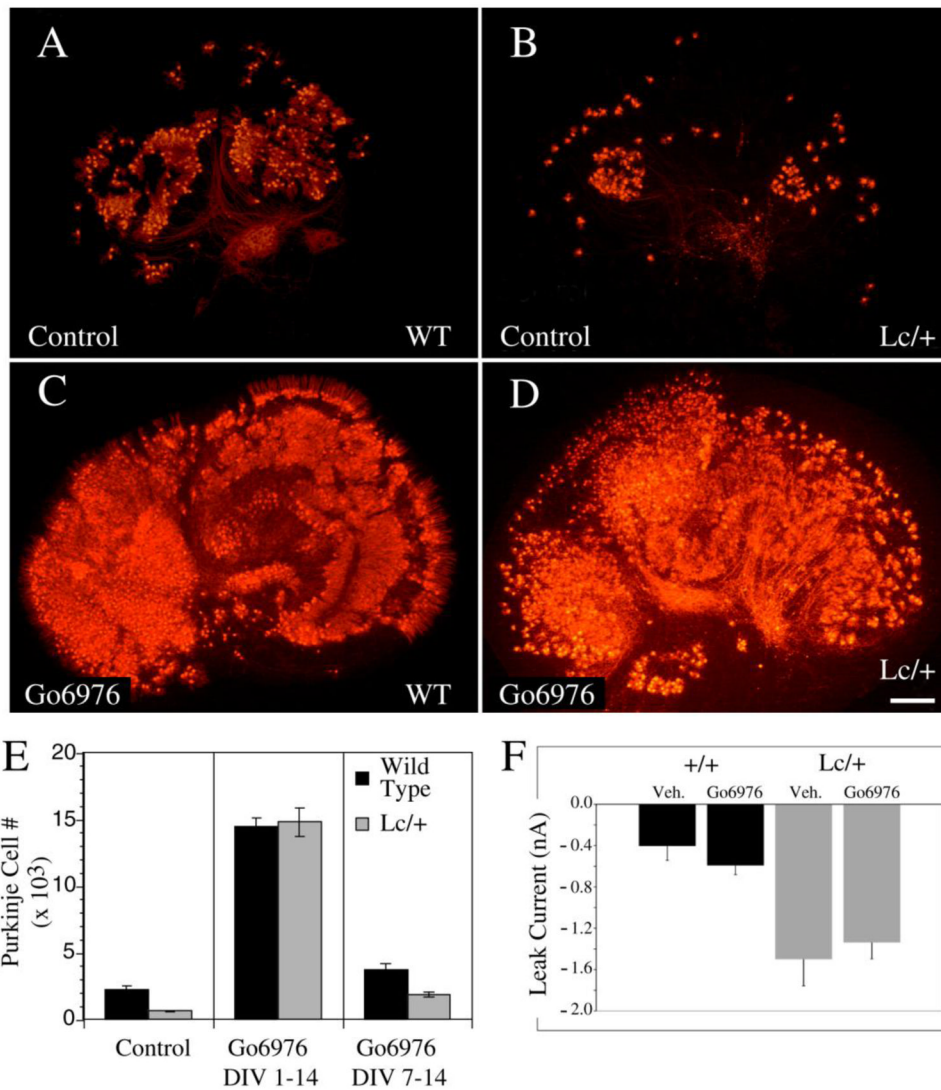


Figure 4.

Treatment of both WT and *Lc/+* cerebellar slice cultures with the conventional PKC inhibitor Gö6976 (1 μ M) from 0 to 14 DIV dramatically increases PC survival. A–D) The images of calbindin labeled control (A and B) and Gö6976-treated (C and D) WT (A, C) and *Lc/+* (B, D) cerebellar slices demonstrates the dramatic increase in the number of surviving PCs after 14 DIV due to ongoing treatment with Gö6976 (Scale bar 200 μ m). E) Treatment with Gö6976 dramatically increases both WT and *Lc/+* PC survival when cultures are treated from the first day in vitro. However, delaying Gö6976 treatment until 7 DIV to 14 DIV still significantly increases WT and *Lc/+* PC survival, although the effects are not as dramatic. F) Measurement of the leak current in WT and *Lc/+* PCs did not show any evidence that treatment with Gö6976 has long term effects on the leak current induced by the mutant GluR82^{Lc} channel. *Lc/+* PCs had larger leak currents whether or not they had been treated with Gö6976.

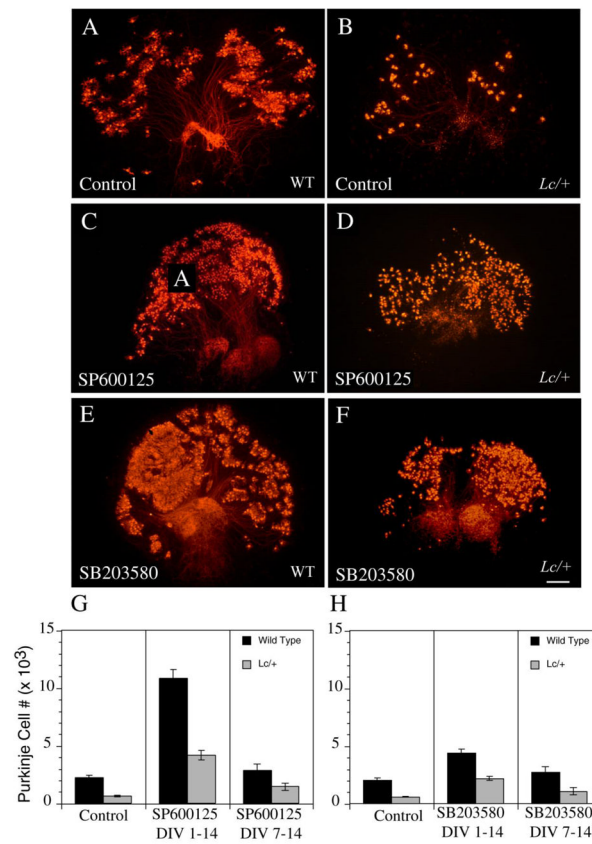


Figure 5.

A) Low magnification images of calbindin immunolabeled WT (A, C, E) and *Lc/+* (B, D, F) cerebellar slice cultures treated with the JNK inhibitor, SP600125, and the p38 inhibitor, SB 203580, demonstrate that both of these inhibitors increase WT and *Lc/+* PC survival when cultures are treated from 0 to 14 DIV. However, the increase in PC survival is not as dramatic as treatment with the cPKC inhibitor Gö6976. G, H) Estimates of total PC numbers in control and drug treated WT and *Lc/+* cerebellar slice cultures from 0 to 14 and 7 to 14 DIV (G: SP600125; H: SB 203580). Scale bar 200 μ m.

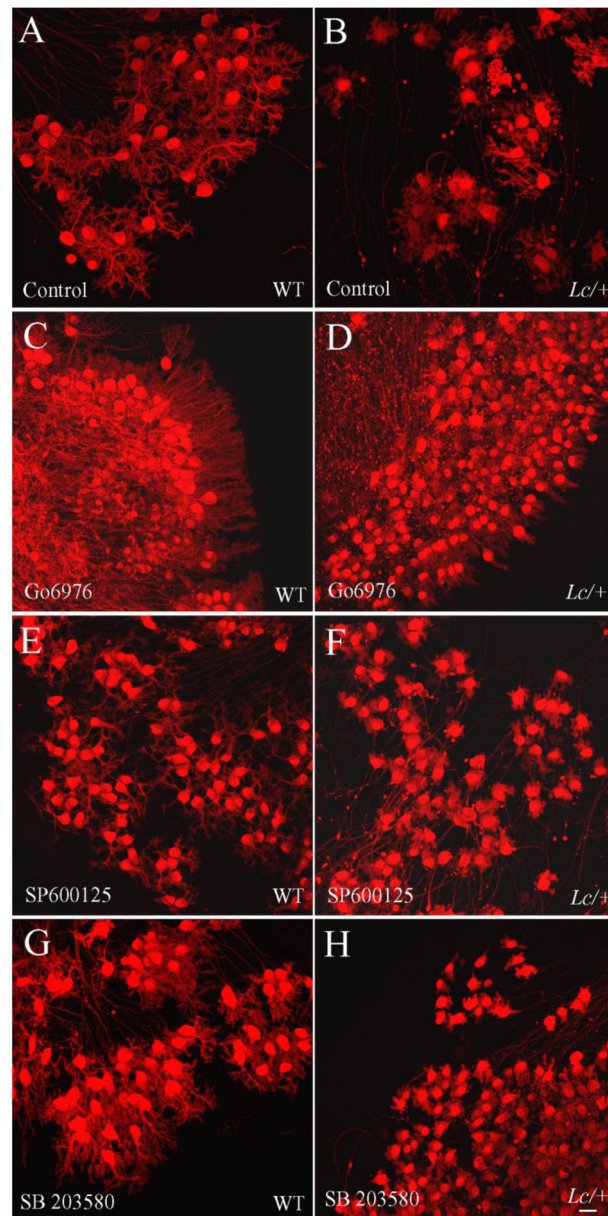


Figure 6. High magnification, confocal images of WT (A, C, E, G) and *Lc/+* (B, D, F, H) PCs in cerebellar slice cultures treated with vehicle (Control) or cPKC, JNK, or p38 inhibitors. The images of the PC dendrites indicate that although the treatment with the three different inhibitors prevented PC death to varying extents, the inhibitors did not affect the stunted dendritic differentiation of *Lc/+* PCs. Scale bar 20 μ m.